Chemical Science

ROYAL SOCIETY OF CHEMISTRY

EDGE ARTICLE

View Article Online
View Journal | View Issue

Cite this: *Chem. Sci.*, 2025, **16**, 10549

All publication charges for this article have been paid for by the Royal Society of Chemistry

Received 29th January 2025
Accepted 18th April 2025

DOI: 10.1039/d5sc00782h

rsc.li/chemical-science

Proximity-induced saccharide binding to a protein's active site within a confined cavity of coordination cages†

Takahiro Nakama, *[a] Miri Tadokoro, [a] Risa Ebihara, [a] Maho Yagi-Utsumi, [bcd] Koichi Kato [bcd] and Makoto Fujita *[ce]

Enhancing protein–ligand affinity is crucial for regulating protein function; however, redesigning ligand molecules often requires extensive trial and error. In this study, we demonstrate proximity-induced ligand binding to a protein's active site by confining it within coordination cages, thereby enabling precise control of protein activity. Co-encapsulation within the confined cavity of the cage brings lysozyme and a low-affinity saccharide into close proximity, resulting in a 10^3-fold decrease in the apparent dissociation constant of the monosaccharide. The significant enhancement of the saccharide binding to the lysozyme active site effectively inhibited its enzymatic activity. NMR studies confirmed the formation of lysozyme–saccharide complexes through enhanced weak interactions, which are otherwise unobservable, facilitated by the confined cavity. This cage confinement strategy thus offers a novel approach for ligand-based functional control of native proteins, eliminating the need for elaborate ligand design and protein engineering.

Introduction

Ligand molecules are generally considered to require high affinity to a protein's active site to regulate protein functions through competitive binding.[1] Interestingly, low-affinity ligands are also often effectively utilized for protein function regulation, as observed in protein–sugar interactions.[2] In such cases, the intracellular confined environment significantly increases the local concentration of ligands, allowing weak protein–ligand interactions with a dissociation constant (K_d) of $\geq 10^{-4}$ to be utilized effectively.[3] In this study, we report that confinement in coordination cages significantly enhances ligand binding to a protein by proximity, allowing for the control of enzymatic activity (Fig. 1). Spherical $M_{12}L_{24}$ coordination cages, self-

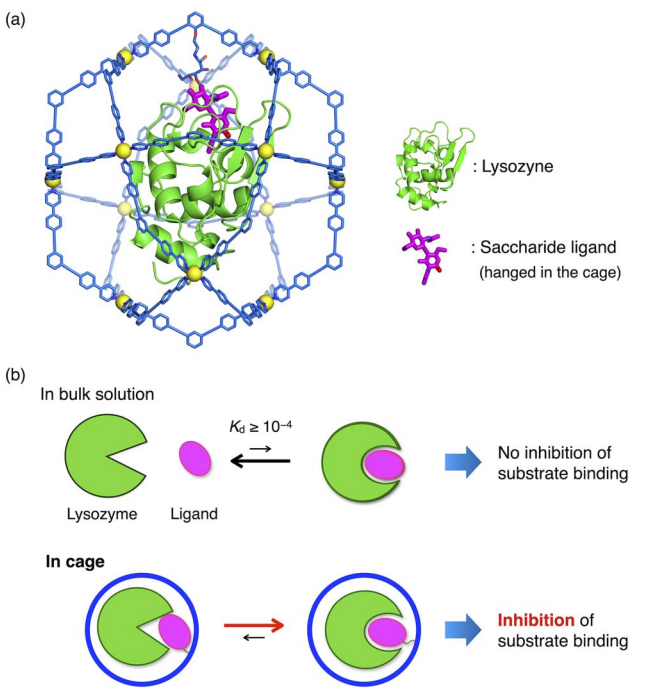

Fig. 1 Enhanced ligand binding to protein's active sites by confinement in coordination cages. (a) Lysozyme–saccharide complex encapsulated in a spherical $M_{12}L_{24}$ coordination cage. (b) Top: Weak ligand binding does not affect protein activities in bulk solutions. Bottom: Proximity within the coordination cage induces the ligand binding to control protein function.

[a]*Department of Applied Chemistry, School of Engineering, The University of Tokyo, Mitsui Link Lab Kashiwanoha 1, FS CREATION, 6-6-2 Kashiwanoha, Kashiwa, Chiba 277-0882, Japan. E-mail: nakama@appchem.t.u-tokyo.ac.jp*

[b]*Exploratory Research Center on Life and Living Systems (ExCELLS), National Institutes of Natural Sciences, 5-1 Higashiyama, Myodaiji, Okazaki, Aichi 444-8787, Japan*

[c]*Institute for Molecular Science (IMS), National Institutes of Natural Sciences, 5-1 Higashiyama, Myodaiji, Okazaki, Aichi 444-8787, Japan*

[d]*Graduate School of Pharmaceutical Sciences, Nagoya City University, 3-1 Tanabe-dori, Mizuho-ku, Nagoya 467-8603, Japan*

[e]*Tokyo College, U-Tokyo Institutes for Advanced Study (UTIAS), The University of Tokyo, 7-3-1 Hongo, Bunkyo-ku, Tokyo 113-0033, Japan. E-mail: mfujita@appchem.t.u-tokyo.ac.jp*

† Electronic supplementary information (ESI) available. See DOI: https://doi.org/10.1039/d5sc00782h

assembled from Pd^{2+} ions (M) and an organic component (L),‡[4] can confine a protein within its well-defined cavity.[5–7] The proximity of a protein and its ligands co-encapsulated in the confined cavity can be enforced by covalently linking the saccharide ligand at the interior of the cages. By confining lysozyme and a low-affinity saccharide in close proximity in the cage, their effective molarity is significantly increased, thereby enhancing the ligand affinity (Fig. 1b). We also show that the weak lysozyme–saccharide complexation, which is otherwise unobservable, can be analyzed by the NMR study thanks to the proximity effect by the confined cavity.

Results and discussion

Proximity of lysozyme and saccharides in coordination cages

To demonstrate the proximity-induced binding within a confined cavity, we encapsulated hen egg-white lysozyme and its low-affinity saccharide ligands, *N*-acetylglucosamine (GlcNAc) or *N*,*N*′-diacetylchitobiose ($(GlcNAc)_2$), in $M_{12}L_{24}$ coordination cages (Fig. 2a and S1†). Saccharide-conjugated organic components **2a** and **2b** were prepared to confine the saccharides using our protein encapsulation scheme[5] (Scheme S1 and Fig. S15–S29†). The N-terminus-selective condensation of lysozyme with the 2-formylpyridyl group[8] of **1** followed by treating with saccharide conjugate **2** and Pd^{2+} ions resulted in the self-assembly of **3** co-encapsulating the protein and saccharides. By this procedure, a single lysozyme molecule can be accommodated along with the saccharides in a well-defined 5.5 nm cavity, as established by our previous studies.[5,6] To achieve a high encapsulation yield, more than two cage equivalents were prepared and the mixture was used directly, as the empty cage does not affect the properties of the encapsulated lysozyme (Fig. S1†).

Diffusion-ordered spectroscopy (DOSY) NMR showed the co-encapsulation of lysozyme and the saccharides in a coordination cage (Fig. 2b, c, S2 and S3†). Upon complexation with Pd^{2+} ions, the ^{1}H NMR spectrum displayed a set of broad signals corresponding to the $M_{12}L_{24}$ cage, lysozyme, and $(GlcNAc)_2$ (Fig. 2b). The diffusion coefficients D for both the protein and saccharide decreased to match that of an empty $M_{12}L_{24}$ cage (Fig. S2,† $D = 1.0 \times 10^{-10}$ m^2 s^{-1}). ^{19}F DOSY NMR selectively detected sugar-conjugated component **2**, indicating a decrease in the D value of the saccharide (Fig. 2c, S2 and S3†). These results, together with the previous analytical ultracentrifugation (AUC) measurements,[5] confirm that both lysozyme and $(GlcNAc)_2$ were confined within the cage.

The statistical arrangement of the saccharide ligands within the cage was demonstrated by electrospray ionization mass spectrometry (ESI-MS, Fig. S5†). When components **1** and **2** were mixed, heteroleptic $M_{12}L_{24}$ cages formed according to the binomial distribution. Consequently, the average number of saccharide ligands in the cage directly reflects the initial mixing ratio (Fig. S1†).

By confining a protein and its ligands within the cage cavity, their proximity is considerably increased, enhancing their effective molarity. Fluorescence resonance energy transfer (FRET) experiments demonstrated this proximity within the coordination cage (Fig. 2d and e). To measure the FRET distance, we labeled lysozyme with the cyanine3 (Cy3) donor

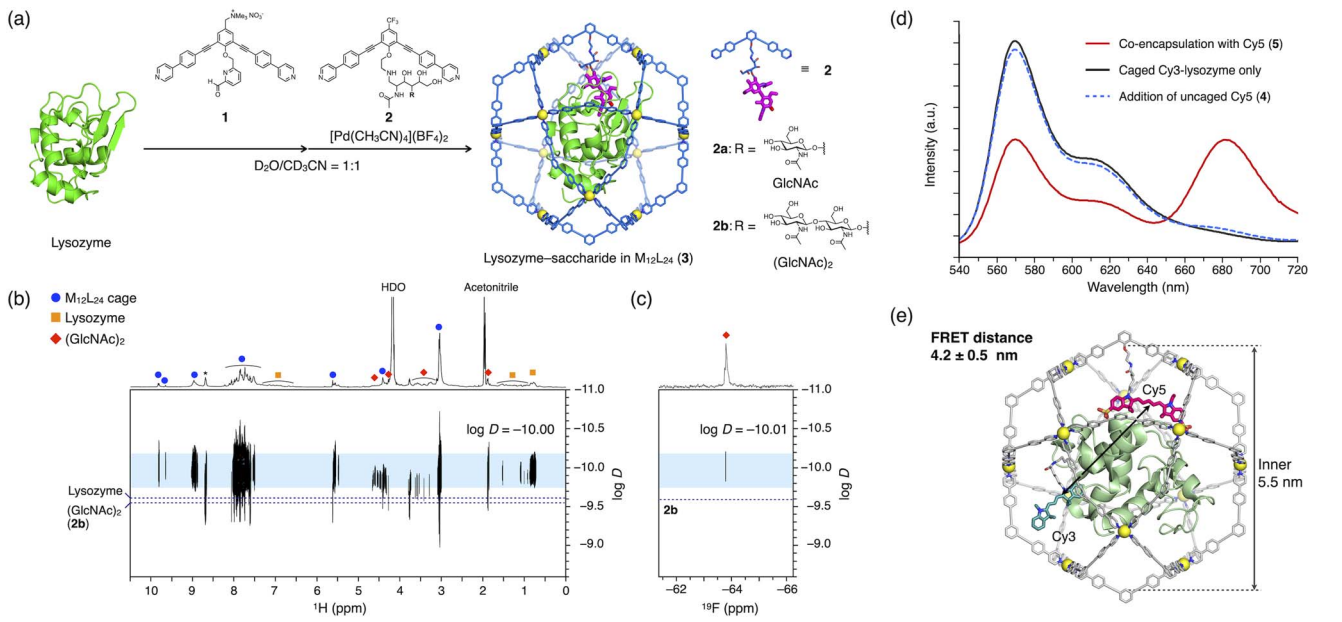

Fig. 2 Co-encapsulation of a protein and ligands in $M_{12}L_{24}$ coordination cages and their proximity in the confined cavity. (a) Schematic representation of co-encapsulation of lysozyme and saccharides GlcNAc or $(GlcNAc)_2$ in the cage. The cage that does not encapsulate lysozyme is omitted for clarity. See Fig. S1† for details. (b) ^{1}H and (c) ^{19}F DOSY NMR spectra of the complex **3b** ((b) 600 MHz, (c) 471 MHz, $D_2O/CD_3CN = 1:1$, 300 K). *Unreacted **1** and **2**. (d) Fluorescence spectra of the Cy3-labeled lysozyme and Cy5 acceptor encapsulated in the cage (complex **5**, red, $\lambda_{ex} = 530$ nm). The spectra of the caged Cy3-lysozyme in the absence (gray) and presence (blue) of free Cy5-conjugate **4** are also shown. (e) Modeling of complex **5**. The FRET distance between Cy3 on lysozyme and Cy5, as well as the cavity diameter, is shown.

and synthesized component **4**, conjugated with the cyanine5 (Cy5) acceptor as a saccharide surrogate (Fig. S5, S30–S33 and Scheme S2†). The Cy3-labeled lysozyme and Cy5 were co-encapsulated in cage **5** (Fig. S4†), and the fluorescence spectra were recorded under Cy3 excitation ($\lambda_{ex} = 530$ nm). This resulted in a strong FRET signal from the Cy5 acceptor ($\lambda_{em} = 681$ nm), accompanied by a decrease in the fluorescence of the Cy3 donor ($\lambda_{em} = 570$ nm) (Fig. 2d and S6, red line†). In contrast, no FRET signal was observed when Cy5-conjugated component **4** was added to the caged lysozyme after encapsulation (blue line).

The FRET distance between the donor and acceptor was calculated to be 4.2 ± 0.5 nm (Fig. 2e; see ESI Notes† for details). This measurement is consistent with the average distance from the periphery of lysozyme to the saccharide ligand within the 5.5 nm diameter cavity. Accordingly, co-encapsulation in the coordination cage facilitates the proximity of the protein and ligands, promoting weak interactions. Due to the stochastic arrangement of the protein and the ligand within the $M_{12}L_{24}$ cages (Fig. S4†), the more ligands encapsulated, the more likely the ligands are to be in close proximity to the protein binding site.

Lysozyme activity inhibition by enhanced saccharide binding in the confined cavity

An inhibition assay of lysozyme activity demonstrated the proximity-induced lysozyme–saccharide interactions (Fig. 3 and S7†). Competitive binding with trisaccharide substrate **6** to the lysozyme active site decreases its enzymatic activity, indicating ligand affinity. Lysozyme activity was assessed by monitoring the fluorescence of the hydrolysis product 4-methylumbelliferone **8** (Fig. 3a).

When GlcNAc or $(GlcNAc)_2$ was added to the caged lysozyme or the uncaged protein, no significant change in its enzymatic activity was observed due to their weak affinities (Fig. 3b(iii) and S7†). Similarly, adding free **2b** did not affect the activity (Fig. 3b(iv)). In contrast, the enzymatic activity of the caged lysozyme was significantly decreased when co-encapsulated with GlcNAc (0.63 ± 0.11) or $(GlcNAc)_2$ (0.59 ± 0.09) (Fig. 3b(i) and (ii), 3.3 saccharides per cage). Therefore, co-encapsulation in the cage enhanced weak lysozyme–saccharide interactions by increasing proximity within the confined cavity.

The apparent dissociation constants $K_{app,d}$ of lysozyme–saccharides within the cage were estimated from the observed decrease in activity. The residual activity was taken to represent the relative reaction rate of lysozyme co-encapsulated with GlcNAc or $(GlcNAc)_2$ compared to that without the ligands. Based on the competitive inhibition in Michaelis–Menten kinetics and the affinity of substrate **6** ($K_d = 2.3 \times 10^{-5}$ M),[9] the $K_{app,d}$ values for GlcNAc and $(GlcNAc)_2$ with lysozyme were determined to be 6.0×10^{-6} M and 5.0×10^{-6} M, respectively (see ESI Notes† for details). These values are significantly lower than the reported dissociation constants of GlcNAc ($K_d = 2.7 \times 10^{-3}$ M)[10] and $(GlcNAc)_2$ ($K_d = 2.7 \times 10^{-4}$ M).[10] In particular, the binding of the monosaccharide GlcNAc in the cage was 4500 times greater than in bulk solutions. The increase in affinity corresponds to the effective molarities of the protein (19 mM) and the saccharide (63 mM) in the 5.5 nm cavity, which are 10^3 times higher than their concentrations under the assay conditions.

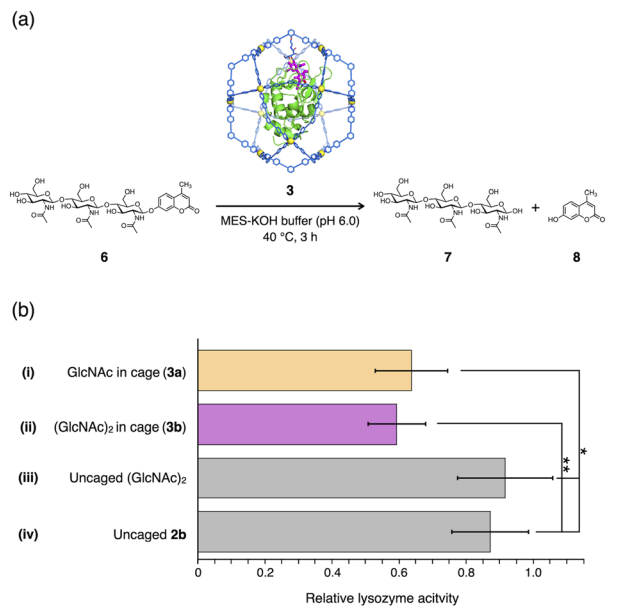

Fig. 3 Proximity-induced saccharide binding to the lysozyme active site in coordination cages to inhibit its enzymatic activity. (a) Schematic representation of the lysozyme activity inhibition assay. (b) Activities of lysozyme co-encapsulated with saccharides ((i) GlcNAc and (ii) $(GlcNAc)_2$), relative to the caged lysozyme without the sugars. The relative activities of the caged lysozyme in the presence of (iii) free $(GlcNAc)_2$ or (iv) free $(GlcNAc)_2$-conjugate **2b** are also shown. [Substrate] = 200 μM, [lysozyme] = 4 μM, [saccharide] = 33 μM, $n = 4$. Error bars indicate standard deviation. Unpaired two-tailed Student's *t*-tests: $*p = 0.02$, $**p = 0.008$.

NMR study of lysozyme–saccharide complexes in coordination cages

NMR spectroscopy shows the binding of saccharides to the lysozyme active site (Fig. 4 and S8–S14†). We employed ^1H–^{13}C selective optimized flip-angle short-transient heteronuclear multiple quantum coherence (SOFAST-HMQC) and heteronuclear single quantum coherence (HSQC) NMR of non-isotope-labeled lysozyme. The spectra, particularly in the methyl and methylene regions, were analyzed to examine the structural changes in lysozyme upon saccharide binding. The caged lysozyme provided ^1H–^{13}C crosspeaks corresponding to its native structure (Fig. S8†).

When lysozyme was co-encapsulated with $(GlcNAc)_2$, minor crosspeaks emerged for some methyl groups in residues at the binding site (I98 and A107), the adjacent helix (I88 and V92), and the hydrophobic core (L17, I55, and M105) (Fig. 4a(i), (ii), b and S9†). The result suggests the conformational alternations in lysozyme upon binding to the saccharide. Notably, minor peak changes were not observed in uncaged lysozyme when $(GlcNAc)_2$ or saccharide-conjugate **2b** was added (Fig. 4a(iii)–(v) and S9†). Titration experiments determined the dissociation constant of $(GlcNAc)_2$ for uncaged lysozyme to be 1.9×10^{-2} M in the water/acetonitrile mixed solvent, requiring a significant excess of the saccharide for its binding (Fig. S14†). In addition,

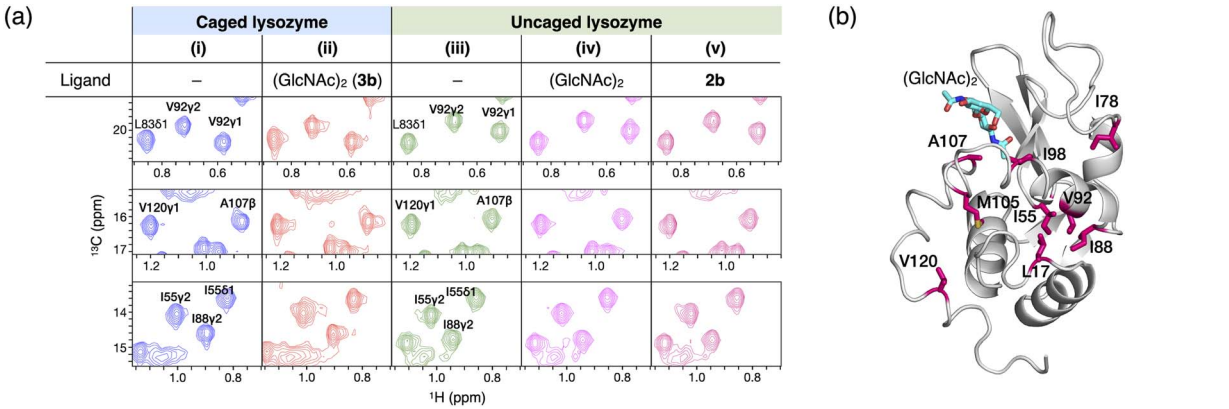

Fig. 4 NMR analysis of the lysozyme–saccharide complex confined in coordination cages. (a) $^{1}H–^{13}C$ SOFAST-HMQC NMR spectra of non-labeled lysozyme co-encapsulated with $(GlcNAc)_2$ (800 MHz, $D_2O/CD_3CN = 1:1$, 300 K). (i) Caged lysozyme without saccharides, (ii) lysozyme co-encapsulated with $(GlcNAc)_2$ in the cage (**3b**), (iii–v) uncaged lysozyme in the (iii) absence and presence of (iv) $(GlcNAc)_2$ or (v) $(GlcNAc)_2$-conjugate **2b**. [Lysozyme] = 200 μM, [$(GlcNAc)_2$] = 1.4 mM. (b) Residues showing a minor HMQC crosspeak by the co-encapsulation are highlighted in magenta on the lysozyme–$(GlcNAc)_2$ structure (PDB 1LZG).

the encapsulation of $(GlcNAc)_2$ led to a reduction in the intensity of HMQC methylene crosspeaks of residues in the hydrophobic core, particularly aromatic residues (Fig. S12†). These results are consistent with the previous NMR studies on lysozyme–saccharide complexes.[11]

$^{1}H–^{13}C$ HMQC spectra also confirm the binding of GlcNAc to lysozyme by encapsulating 12 molecules of the monosaccharide in the cage (Fig. S10 and S11†). The appearance of the minor methyl peak was observed to be similar to the binding with $(GlcNAc)_2$. Without encapsulation in the cage, even the addition of 300 eq. GlcNAc (180 mM), close to its saturation concentration, did not result in similar spectral changes (Fig. S14†). Accordingly, confinement in the coordination cages significantly enhanced the binding of the saccharides to the lysozyme active site, allowing the control of its enzymatic activity. In addition, the NMR studies of lysozyme–saccharide complexes in the cage suggest that the co-encapsulation can be utilized for structural analysis of such transient protein–ligand complexes.

Conclusions

In summary, this study presents an approach to enhance ligand affinity for regulating protein function by confinement in coordination cages. When saccharides were co-encapsulated with lysozyme in a confined cavity of $M_{12}L_{24}$ spherical cages, the enforced proximity induced the weak binding ($K_d \geq 10^{-4}$) to the protein active site, effectively competing with a higher affinity substrate. The activity decrease corresponds to a 10^3-fold enhancement of the saccharide binding, consistent with the increase in the effective molarity within the cage. NMR analysis demonstrated the enhanced binding of saccharides to the lysozyme catalytic site.

While such confinement effects in host cavities have been widely discussed for complexes of small molecules,[12] they have never been investigated for protein–ligand complexes due to the lack of suitable host matrices capable of arranging them in nanometer-sized cavities.[13] A well-defined, designable cavity of $M_{12}L_{24}$ coordination cages is ideal for the proximity-induced ligand binding to control protein function, in contrast to the heterogeneous cavities of conventional hosts.[14]

This confinement strategy can be applied directly to native proteins without the need for mutations or elaborate ligand modification. This approach also offers an advantage over direct protein–ligand conjugation, which requires careful control over linker design and conjugation sites.[15] Weak natural ligands, such as saccharides, can be repurposed as an effector with over 1000 times greater affinity. This would enable not only competitive binding but also allosteric regulation[16] of proteins. Consequently, confinement in the coordination cage can be a practical strategy for modulating protein functions.

Data availability

The data supporting this article have been included as part of the ESI.†

Author contributions

Conceptualization, T. N. and M. F.; methodology, T. N., M. T., M. Y.-U., and K. K.; investigation, T. N., M. T., R. E., and M. Y.-U.; visualization, T. N.; funding acquisition, T. N., M. Y.-U., and M. F.; project administration, T. N. and M. F.; resources, T. N., M. Y.-U. K. K., and M. F.; supervision, T. N. and M. F.; writing – original draft: T. N. and M. F.; writing – review & editing: T. N., M. T., R. E., M. Y.-U., K. K., and M. F.

Conflicts of interest

The authors declare no competing interests.

Acknowledgements

This research was supported by JSPS Grants-in-Aid for Specially Promoted Research (JP19H05461 to M. F.), JSPS Grants-in-Aid

Early-Career Scientists (JP21K14640 and JP25K18122 to T. N.), JST PRESTO (JPMJPR22AC to M. Y.-U.), and Joint Research of the ExCELLS (24EXC317 and 23EXC314 to T. N.). R. E. acknowledges a JSPS Research Fellowship for Young Scientists (23KJ0670). T. N. thanks the Japan Science Society and the Iketani Science and Technology Foundation for financial support. The NMR experiments performed at ExCELLS were supported by MEXT NMR Platform and by MEXT Promotion of Development of a Joint Usage/Research System Project: CURE (JPMXP 1323015488, Spin-L Program No. spin23XN019, spin24XN007 to T. N.). We also thank Dr Nishikawa (JEOL Ltd.) for technical assistance with ^{19}F DOSY NMR measurements.

Notes and references

‡ Organic molecules that coordinate to metals are referred to as "ligands" in chemical terminology. To avoid confusion with protein "ligands", the chemical ligands such as **2** and related compounds are referred to as the term "organic component" or simply "component" throughout this manuscript (though they are abbreviated as L in describing the $M_{12}L_{24}$ cages).

1 (*a*) A. A. Sadybekov, A. V. Sadybekov, Y. Liu, C. Iliopoulos-Tsoutsouvas, X. P. Huang, J. Pickett, B. Houser, N. Patel, N. K. Tran, F. Tong, N. Zvonok, M. K. Jain, O. Savych, D. S. Radchenko, S. P. Nikas, N. A. Petasis, Y. S. Moroz, B. L. Roth, A. Makriyannis and V. Katritch, *Nature*, 2022, **601**, 452–459; (*b*) X. Du, Y. Li, Y. L. Xia, S. M. Ai, J. Liang, P. Sang, X. L. Ji and S. Q. Liu, *Int. J. Mol. Sci.*, 2016, **17**, 144; (*c*) A. Stank, D. B. Kokh, J. C. Fuller and R. C. Wade, *Acc. Chem. Res.*, 2016, **49**, 809–815.

2 (*a*) K. Furukawa, Y. Ohkawa, Y. Yamauchi, K. Hamamura, Y. Ohmi and K. Furukawa, *J. Biochem.*, 2012, **151**, 573–578; (*b*) Y. van Kooyk and G. A. Rabinovich, *Nat. Immunol.*, 2008, **9**, 593–601.

3 (*a*) K. G. Hicks, A. A. Cluntun, H. L. Schubert, S. R. Hackett, J. A. Berg, P. G. Leonard, M. A. A. Aleixo, Y. Zhou, A. J. Bott, S. R. Salvatore, F. Chang, A. Blevins, P. Barta, S. Tilley, A. Leifer, A. Guzman, A. Arok, S. Fogarty, J. M. Winter, H. C. Ahn, K. N. Allen, S. Block, I. A. Cardoso, J. Ding, I. Dreveny, W. C. Gasper, Q. Ho, A. Matsuura, M. J. Palladino, S. Prajapati, P. Sun, K. Tittmann, D. R. Tolan, J. Unterlass, A. P. VanDemark, M. G. Vander Heiden, B. A. Webb, C. H. Yun, P. Zhao, B. Wang, F. J. Schopfer, C. P. Hill, M. C. Nonato, F. L. Muller, J. E. Cox and J. Rutter, *Science*, 2023, **379**, 996–1003; (*b*) I. Piazza, K. Kochanowski, V. Cappelletti, T. Fuhrer, E. Noor, U. Sauer and P. Picotti, *Cell*, 2018, **172**, 358–372; (*c*) P. Tompa, N. E. Davey, T. J. Gibson and M. M. Babu, *Mol. Cell*, 2014, **55**, 161–169; (*d*) F. X. Theillet, A. Binolfi, T. Frembgen-Kesner, K. Hingorani, M. Sarkar, C. Kyne, C. Li, P. B. Crowley, L. Gierasch, G. J. Pielak, A. H. Elcock, A. Gershenson and P. Selenko, *Chem. Rev.*, 2014, **114**, 6661–6714.

4 (*a*) K. Harris, D. Fujita and M. Fujita, *Chem. Commun.*, 2013, **49**, 6703–6712; (*b*) M. Tominaga, K. Suzuki, M. Kawano, T. Kusukawa, T. Ozeki, S. Sakamoto, K. Yamaguchi and M. Fujita, *Angew. Chem., Int. Ed.*, 2004, **43**, 5621–5625.

5 R. Ebihara, T. Nakama, K. Morishima, M. Yagi-Utsumi, M. Sugiyama, D. Fujita, S. Sato and M. Fujita, *Angew. Chem., Int. Ed.*, 2025, **64**, e202419476.

6 (*a*) T. Nakama, A. Rossen, R. Ebihara, M. Yagi-Utsumi, D. Fujita, K. Kato, S. Sato and M. Fujita, *Chem. Sci.*, 2023, **14**, 2910–2914; (*b*) D. Fujita, R. Suzuki, Y. Fujii, M. Yamada, T. Nakama, A. Matsugami, F. Hayashi, J.-K. Weng, M. Yagi-Utsumi and M. Fujita, *Chem*, 2021, **7**, 2672–2683.

7 (*a*) H. Tamura, T. Nakama, A. Rossen, H. Ishikita and M. Fujita, *Chem. Lett.*, 2024, **53**, upae101; (*b*) D. Fujita, K. Suzuki, S. Sato, M. Yagi-Utsumi, Y. Yamaguchi, N. Mizuno, T. Kumasaka, M. Takata, M. Noda, S. Uchiyama, K. Kato and M. Fujita, *Nat. Commun.*, 2012, **3**, 1093.

8 J. I. Macdonald, H. K. Munch, T. Moore and M. B. Francis, *Nat. Chem. Biol.*, 2015, **11**, 326–331.

9 Y. Yang and K. Hamaguchi, *J. Biochem.*, 1980, **88**, 829–836.

10 J. Landström, M. Bergström, C. Hamark, S. Ohlson and G. Widmalm, *Org. Biomol. Chem.*, 2012, **10**, 3019–3032.

11 (*a*) S. Mine, S. Tate, T. Ueda, M. Kainosho and T. Imoto, *J. Mol. Biol.*, 1999, **286**, 1547–1565; (*b*) A. Kristiansen, K. M. Varum and H. Grasdalen, *Eur. J. Biochem.*, 1998, **251**, 335–342; (*c*) T. Fukamizo, Y. Ikeda, T. Ohkawa and S. Goto, *Eur. J. Biochem.*, 1992, **210**, 351–357; (*d*) T. Ueda, Y. Isakari, H. Aoki, T. Yasukochi, S. Masutomo, K. Kawano, Y. Terada, H. Yamada and T. Imoto, *J. Biochem.*, 1991, **109**, 690–698.

12 (*a*) A. B. Grommet, M. Feller and R. Klajn, *Nat. Nanotechnol.*, 2020, **15**, 256–271; (*b*) S. M. Treacy, A. L. Smith, R. G. Bergman, K. N. Raymond and F. D. Toste, *J. Am. Chem. Soc.*, 2024, **146**, 29792–29800; (*c*) S. Y. Liu, N. Kishida, J. Kim, N. Fukui, R. Haruki, Y. Niwa, R. Kumai, D. Kim, M. Yoshizawa and H. Shinokubo, *J. Am. Chem. Soc.*, 2023, **145**, 2135–2141; (*d*) F. J. Rizzuto, L. K. S. von Krbek and J. R. Nitschke, *Nat. Rev. Chem.*, 2019, **3**, 204–222.

13 (*a*) T. G. W. Edwardson, M. D. Levasseur, S. Tetter, A. Steinauer, M. Hori and D. Hilvert, *Chem. Rev.*, 2022, **122**, 9145–9197; (*b*) W. Liang, P. Wied, F. Carraro, C. J. Sumby, B. Nidetzky, C. K. Tsung, P. Falcaro and C. J. Doonan, *Chem. Rev.*, 2021, **121**, 1077–1129; (*c*) M. Vázquez-González, C. Wang and I. Willner, *Nat. Catal.*, 2020, **3**, 256–273; (*d*) Y. Chen, P. Li, J. Zhou, C. T. Buru, L. Aorević, P. Li, X. Zhang, M. M. Cetin, J. F. Stoddart, S. I. Stupp, M. R. Wasielewski and O. K. Farha, *J. Am. Chem. Soc.*, 2020, **142**, 1768–1773; (*e*) A. Küchler, M. Yoshimoto, S. Luginbühl, F. Mavelli and P. Walde, *Nat. Nanotechnol.*, 2016, **11**, 409–420; (*f*) W. C. B. McTigue and S. L. Perry, *Small*, 2020, **16**, 1907671; (*g*) Y. Zhang and H. Hess, *Chin. J. Chem. Eng.*, 2020, **28**, 2028–2036; (*h*) D. J. McClements, *Adv. Colloid Interface Sci.*, 2018, **253**, 1–22.

14 (*a*) Y. R. Maghraby, R. M. EI-Shabasy, A. H. Ibrahim, H. M and E. Azzazy, *ACS Omega*, 2023, **8**, 5184–5196; (*b*) L. van der Koog, T. B. Gandek and A. Nagelkerke, *Adv. Healthcare Mater.*, 2022, **11**, 2100639; (*c*) A. Rodriguez-Abetxuko, D. Sánchez-deAlcázar, P. Muñumer and A. Beloqui, *Front. Bioeng. Biotechnol.*, 2020, **8**, 830; (*d*) R. Chapman and M. H. Stenzel, *J. Am. Chem. Soc.*, 2019, **141**, 2754–2769; (*e*)

E. Rideau, R. Dimova, P. Schwille, F. R. Wurm and K. Landfester, *Chem. Soc. Rev.*, 2018, **47**, 8572–8610; (*f*) B. Panganiban, B. Qiao, T. Jiang, C. Delre, M. M. Obadia, T. D. Nguyen, A. A. A. Smith, A. Hall, I. Sit, M. G. Crosby, P. B. Dennis, E. Drockenmuller, M. Olvera, D. Cruz and T. Xu, *Science*, 2018, **359**, 1239–1243; (*g*) Z. Zhou and M. Hartmann, *Chem. Soc. Rev.*, 2013, **42**, 3894–3912; (*h*) K. F. O'Driscoll, *Methods Enzymol.*, 1976, **44**, 169–183.

15 V. M. Krishnamurthy, V. Semetey, P. J. Bracher, N. Shen and G. M. Whitesides, *J. Am. Chem. Soc.*, 2007, **129**, 1312–1320.

16 (*a*) J. Guo and H. X. Zhou, *Chem. Rev.*, 2016, **116**, 6503–6515; (*b*) N. M. Goodey and S. J. Benkovic, *Nat. Chem. Biol.*, 2008, **4**, 474–482; (*c*) A. Chatzigoulas and Z. Cournia, *Wiley Interdiscip. Rev.: Comput. Mol. Sci.*, 2021, **11**, e1529.